

25 **Abstract**

26 Development of a safe, effective and inexpensive therapy for African trypanosomiasis is an
27 urgent priority. In this study, we evaluate the validity of *T. brucei* glycogen synthase kinase 3 (GSK-3) as
28 potential drug target. RNA interference of either of two GSK-3 homologues in bloodstream form *T.*
29 *brucei* led to growth arrest and altered parasite morphology, demonstrating their requirement for cell
30 survival. Since the growth arrest after RNAi appeared more profound for *Tbru*GSK-3 “short”
31 (Tb10.161.3140) vs. *Tbru*GSK-3 “long” (Tb927.7.2420), we focused on *Tbru*GSK-3 short for further
32 studies. *Tbru*GSK-3 short with an N-terminal maltose-binding protein fusion was cloned, expressed and
33 purified in a functional form. The potency of a GSK-3-focused inhibitor library against recombinant
34 enzyme of *Tbru*GSK-3 short, as well as bloodstream form parasites was evaluated with the aim of
35 determining if compounds inhibiting enzyme activity could also block parasites’ growth and proliferation.
36 Among the cell active compounds, there was an excellent correlation of activity inhibiting *Tbru*GSK short
37 enzyme and inhibition of *T. brucei* growth. Thus there is reasonable genetic and chemical validation of
38 GSK-3 short as a drug target for *T. brucei*. Finally, selective inhibition may be required for therapy
39 targeting the GSK-3 enzyme, and a molecular model of *Tbru*GSK short enzyme suggests that compounds
40 can be found that selectively inhibit *Tbru*GSK-3 short over the human GSK-3 enzymes.

41
42
43
44
45
46
47
48
49
50

Introduction

The vector borne parasitic disease, African trypanosomiasis, caused by *Trypanosoma brucei* complex, is a serious health threat. It is estimated that 300,000-500,000 humans are infected in sub-Saharan African. If left inadequately treated, the disease often has a fatal outcome (9). Safe and effective therapy, once infection is established, is critically important, yet has been difficult to achieve. Despite the critical need, available therapies are becoming less satisfactory due to the rising level of resistance to available drugs, the long period of treatment required to achieve cure, and the unacceptable and sometimes severe adverse effects associated with current therapies (9). An urgent priority is to identify and validate new targets for development of safe, effective and inexpensive therapeutic alternatives.

Recent advances in the area of parasite genomics and biochemical investigation of physiologically important enzymes necessary for the parasite's survival have identified protein kinases as potential drug targets for trypanosomatid diseases (3,14,23). Protein kinases play an important role in cell survival by phosphorylating and regulating many activities of the cell, including protein synthesis, gene expression, subcellular localization of proteins, and protein degradation machinery. Many kinases have been examined for the physiological relevance of their phosphorylation activities in other organisms, and glycogen synthase kinase 3 (GSK-3) has been found to be essential in many fundamental cellular processes (22,30).

Far from being simply important in glycogen synthesis, GSK-3 activity is now recognized as key in mammalian cells signaling pathways for many cellular and physiological events (26). GSK-3 has been targeted for treatment of several diseases, such as diabetes mellitus and Alzheimer's dementia, and this enzyme has been found to be amenable to selective targeting with small molecule drugs (22). GSK-3 has two isoforms in human cells, GSK-3 α and GSK-3 β . GSK3 α and GSK3 β isoforms rarely diverge outside the N- and C-terminal regions. Within the ATP binding site of GSK3, where most GSK-3 inhibitors bind, there appears to be only a single amino acid difference (Glu196 in GSK3 α , Asp133 in GSK3 β), and most inhibitors target both isoforms. GSK-3 generally requires a substrate that is pre-phosphorylated by a

76 priming kinase (6,7,10,32) (Fig. 1), leading to a role in signaling cascades. GSK-3 is regulated by auto-
77 phosphorylation and phosphorylation by other enzymes.

78 Even though orthologues exhibit a high degree of sequence similarity within their catalytic
79 domains (7, 22), there exists evolutionary differences between human and parasite homologues that might
80 be sufficient to allow the design of parasite-specific inhibitors. Compounds that inhibit *T. brucei* GSK-3
81 activity and not host GSK-3 might be required for therapy of pregnant women and infants in that GSK-3
82 regulates proteins critical in development such as the *wnt* gene product. However, optimization of the
83 selectivity of drug candidates for parasite kinases becomes an issue due to the highly conserved amino
84 acids and protein conformation of the catalytic domains (5,18,25,26). Understanding the differences in
85 substrate binding properties and 3-dimensional structures between mammalian and parasite GSK-3 is
86 important for optimization of selected target inhibitors for drug development (6,18).

87 In this report, we show by RNAi assay and chemical validation that *Tbru*GSK3 is a potential drug
88 target for treatment of African sleeping sickness. Inhibitor-target interactions, expressed as calculated
89 interaction energy could be predicted and improved upon using computer modeling software to detect
90 binding pockets present in *Tbru*GSK-3 but absent in the human homologue of the enzyme (18).

91 92 **Materials and Methods**

93 **Bioinformatics-***T. brucei* orthologs to the human GSK-3 α (UniProt P49840) and human GSK-3 β
94 (UniProt P49841) were identified in the *T. brucei* genome using the BLASTP tool on the web site
95 GeneDB (www. Genedb.org). Amino acid identity values were determined using the ALIGN tool (24) on
96 the Biology Workbench 3.2 website (<http://segtool.sdsc.edu/CGI/BW.cgi>).

97
98 **RNA interference-** The two *Tbru*GSK-3 homologs, encoding a long and a short isoform of the
99 enzyme, were targets for the knock-down experiment. Two RNAi constructs were made to knock-down
100 the short gene and one for the longer isoform. Selection of regions within *Tbru*GSK-3 short and long gene
101 coding sequences for RNAi plasmid constructs was determined using the RNA target selection program

102 RNAi (29) to ensure that there was no significant sequence homology with other genes within the
103 genome. Sequences of *T. brucei* genomic DNA used in the construction of RNAi plasmids were taken
104 from GeneDB accession nos. Tb10.61.3140 (*Tbru*GSK-3 short, nucleotides 176-578 for construct 1 and
105 665-1056 for construct 2) and Tb927.7.2420 (*T. brucei* long, nucleotides 159-531), respectively.
106 Nucleotide bases between primer pairs (1 and 2; 3 and 4; 5 and 6 see Table 5) were amplified from
107 *T. brucei* 927 genomic DNA. Resultant amplicons were ligated using TA cloning into the vector
108 p2T7^{TAB_{lue}} (2) (gift of D. Horn, London School of Hygiene and Tropical Medicine) and confirmed by
109 nucleotide sequence analysis of inserts. The constructs were linearized with *NotI* restriction enzyme (New
110 England Biolabs, Ipswich, MA). *T. brucei* bloodstream-form parasites (provided by G. Cross,
111 Rockefeller University) expressing the T7 RNA polymerase and Tet repressor under single selection
112 marker, G418 resistance, (single marker, SM) were cultured in HMI-9 with 10% heat-inactivated fetal
113 bovine serum at 37°C and 5% CO₂ with G418 at 2.5 µg/ml (15). Ten micrograms (10 µg) of linearized
114 p2T7^{TAB_{lue}}/*Tbru*GSK-3 were electroporated into mid-log phase *T. brucei* (2.5×10^7) suspended in 500 µl
115 of cytomix (120 mM KCl, 0.15 mM CaCl₂, 10 mM K₂HPO₄/KH₂PO₄ pH 7.6, 25 mM HEPES, 2 mM
116 Na₂EDTA, 5 mM MgCl₂). Electroporation was done in 4 mm gap cuvettes at 1.6 kV and 24 Ω as
117 described (33). Cells were re-suspended in HMI-9 medium supplemented with 2.5 µg/ml hygromycin and
118 2.5 µg/ml G418. Stable individual clones were selected 5-7 days after transfection. Selected cultures
119 diluted to 1×10^5 cells/ml were induced for double-stranded RNA expression by addition of 1 µg/ml
120 tetracycline. Growth was measured in cultures passed daily at a 1:10-1:20 dilution and monitored using
121 ATPLite Luminescence ATP Detection Assay System (cat #6016941, PerkinElmer, Waltham, MA). Cell
122 growth was monitored for 7 days.

123
124 **Northern analysis-** RNA was isolated from induced and non-induced cultures after 48 hours of growth
125 using the RNEasy kit (Qiagen, Valencia, CA). Twelve to sixteen micrograms (12-16 µg) of total RNA
126 was electrophoresed on a formaldehyde gel and blotted using standard procedures (4). The RNA
127 membrane was then analyzed with a ³²P-labeled-DNA probe complementary to GSK-3 mRNA from a

128 region not contained in the RNAi constructs. The probe was amplified from genomic DNA using the
129 primers: 3 and 4 for GSK Short-1, primers 1 and 2 for GSK Short-2 and primers 7 and 8 for GSK long
130 (Table 5).

131
132 **DNA-DNA Hybridization-** Genomic DNA was isolated from *T. brucei* 427 by lysis in TELT buffer
133 (50 mM Tris/HCl, pH 8.0/62.5 mM EDTA/2.5 M LiCl/49% (v/v) Triton X-100), followed by a phenol-
134 Chloroform extraction (20) and subjected to double restriction endonuclease digests. Enzymes were
135 picked in the regions outside the gene of interest that would cut about 1000 bp outside the genes.
136 Restricted fragments ran on 1.0 % agarose gel were visualized after staining with ethidium bromide and
137 subsequently blotted to a nitrocellulose membrane (Amersham Pharmacia Biotech, Buckinghamshire
138 England) by capillary transfer. The membrane was probed with appropriately ³²P -radiolabeled RNAi
139 region for the GSKShort-1 gene amplified with primer pairs 1 and 2 (Table 5).

140
141 **Polymerase chain reaction and ligase independent cloning (LIC)-** Regions of *Tbru*GSK-3 short gene
142 ORF were amplified from *T. brucei* 427 genomic DNA using the primers *Tbru*GSKFwd , *Tbru*GSKRev
143 [9 and 10 (Table 5)]. Primer and probe sequences used in this study are listed in Table 5. The PCR
144 product cloned into the maltose-binding-protein-fusion-(MBP)-AVA0421- vector. MBP-AVA0421 is a
145 ligase-independent-cloning (LIC) vector that expresses proteins as N-terminal 6-His-MBP-3C cleavage
146 site-ORF fusion. The AVA0421-MBP was generated from AVA0421 by ligating the PCR-amplified
147 MBP sequence from 8-His-MBP-BG1861 between NdeI and KpnI restrictions sites (1). The inserts and
148 *NruI-PmeI* double digested vector were ligated using ligase independent cloning (LIC) as previously
149 described (21).

150
151 **Expression and Purification of *T. brucei* GSK-3 short version-** Expression of recombinant protein using
152 BL21(DE5)* (Invitrogen, Carlsbad, CA) was auto induced in ZY5052 media supplemented with
153 100µg/ml ampicillin grown for 24 hours at 20°C and 200 rpm agitation. Cells were harvested by

154 centrifugation and stored at -80°C after flash freezing in liquid nitrogen. Frozen cells were resuspended
155 and disrupted with sonication in 200 ml lysis buffer containing 25 mM HEPES (pH 7.25), 500 mM NaCl,
156 5% glycerol, 2 mM DTT (standard buffer), 10 mg lysozyme with 20 mM Imidazole. Cell debris was
157 clarified by centrifugation while target protein was purified from the clarified cell lysate by binding on
158 standard buffer equilibrated NTA nickel resins (Qiagen, Valencia, CA). Recombinant *Tbru*GSK-3 short
159 protein was eluted in 250 mM imidazole plus 1 mM DTT and dialysed in standard buffer with 1 mM DTT
160 and was further resolved by size exclusion gel chromatography [Superdex 75 26/60, (GE Biosciences,
161 Piscataway, NJ)]. Pure fractions collected as a single peak were analyzed by Biorad Gel code blue -
162 stained SDS-PAGE analysis (Fig. 4). Enzyme storage condition was -20°C in 50% glycerol, 12.5 μM
163 Hepes pH 7.5, 250 μM NaCl, 0.5 μM DTT, 0.0125% Sodium azide and 1 X protease inhibitor (Roche,
164 Indianapolis, IN).

166 **Chemical Inhibitors.** GW8510 [Sigma Chemical Co., St. Louis, MO] (16), SU9516 [Sigma
167 Chemical Co., St. Louis, MO] (22), SB-415286 [BIOMOL., Plymouth Meeting, PA] (22), Cdk1/2
168 Inhibitor III [Calbiochem, San Diego, CA] (8), 2-Cyanoethyl Alsterpauellone [Calbiochem, San Diego,
169 CA] (17) (Table 3) and 43 other commercially available protein kinase inhibitors [Sigma, Biomol, &
170 Calbiochem] were included in this study. In addition, a 255 compound GSK-3 focused library
171 collection obtained from Merck-Serono Inc. was also evaluated. Most of the Merck-Serono
172 GSK-3 inhibitors have a 2(Z)-2-(4-*tert*-butylthiazol-2(3*H*)-ylidene)-2-(2-aminopyrimidin-4-yl)
173 acetonitrile core structure with modifications (R1) as shown in Table 4.

174 **Activity assay-** Enzyme activity was measured in a Scintillation Proximity Assay (SPA) using streptavidin
175 coated Beads, [γ -³³P] ATP (Amersham Biosciences Corps, Piscataway, NJ), and biotinylated peptide
176 substrate (BioGSP-2. Peptide sequence: Biotin-C6-Tyr-Arg-Arg-Ala-Ala-Val-Pro-Pro-Ser-Pro-Ser-Leu-
177 Ser-Arg-His-Ser-Ser-Pro-His-Gln-Ser(PO₃H₂)-Glu-Asp-Glu-Glu-Glu) (American Peptide Company, Inc.
178 Sunnyvale, CA). A filtration assay was used to measure specific-activity of GSK-3 and the Km for ATP

179 and the peptide substrate (BioGSP-2), measuring the incorporation of [γ -³³P] into the peptide and its
180 subsequent binding to a P-81 filter (Whatman, Florhan Park, NJ). All assays were performed in a buffered
181 solution containing 25 mM Tris-HCl (pH 7.5), 10 mM MgCl₂·6H₂O, 5 mM DTT, 0.1 mg/mL BSA plus 2
182 U/mL Heparin and incubated at 30°C. The filtration assay reaction volume of 50 μ l containing 1.2 μ M
183 BioGSP-2, serially diluted enzyme concentrations, unlabeled (1.2 μ M) and [γ -³³P] labeled ATP (4 nM)
184 was incubated for 60 minutes. Reactions were stopped with 100 μ l of 10% Trifluoroacetic acid in 37.5
185 mM EDTA and 750 μ M unlabeled ATP. The content of each was spotted on P81 filters and washed 3
186 times in 2.5% Phosphoric acid. The SPA assay was used for inhibitor screening and determining IC₅₀
187 values of 303 inhibitors against *Tbru*GSK-3 short at the Km determined for ATP and peptide. The SPA
188 assay mix included 20 ng (46.8 nM) of enzyme, 2.4 μ M of peptide substrate, 4.5 μ M unlabeled ATP and
189 4 nM [γ -³³P] labeled ATP. The reaction was incubated for 30 minutes. Quantitative measurement of
190 phosphate incorporation and binding to BioGSP-2 by *Tbru*GSK-3 short enzyme was determined using
191 100 μ l of 20 mg/mL streptavidin coated SPA beads in 37.5 mM EDTA and 75 μ M unlabeled ATP. In
192 each assay, human GSK-3 β (Upstate Cell Signaling Solutions, Temecula CA) and assay buffer were used
193 as positive and negative controls respectively. Emission of light by this SPA beads simulation reaction
194 was measured as counts per minute on the Chameleon 425-104 multi-label plate scintillation counter
195 (Hidex, Oy, Turku Finland).

196

197 ***Parasite Cultures and in vitro Compound Screening Assays***- Bloodstream-form *T. brucei brucei* strain
198 427 was cultured in HMI-9 medium supplemented with 10% heat-deactivated fetal bovine serum, 1%
199 penicillin and streptomycin at 37°C in 5% CO₂ supply as earlier described (15). *In-vitro* susceptibility to
200 compounds was tested in 96 well plates with an initial inoculum size of 1 \times 10⁵ trypomastigotes per well.
201 Compound stock solutions were prepared in DMSO at 10-20 mM and diluted in HMI-9 medium to 20
202 μ M, then added in serial dilutions for a final volume of 200 μ L/well. Growth of triplicate cultures was
203 quantitated after 48 hours by the addition of Alamar Blue (Alamar Biosciences, Sacramento, CA) (28).

204 Pentamidine isethionate (Aventis, Dagenham, UK) was included in each assay as a positive control. The
205 effective concentration which causes 50% growth inhibition values (EC_{50}) was calculated using nonlinear
206 regression in Prism (Graphpad Software, Inc. La Jolla, CA).

207
208 **Homology modeling of *T. brucei* GSK-3 and inhibitor docking-** The Protein Data Bank (PDB)
209 contains 14 structures of human GSK, each with variations in the hinge domain motion between
210 the N- and C-terminal lobes of the enzyme. For modeling the 3D structure of *Tbru*GSK-3 short,
211 PDB 1R0E, human GSK-3 complexed with a 3-indolyl-4-arylmaleimide inhibitor was ultimately
212 chosen as the template because the resulting model led to the best Quantitative Structure-Activity
213 Relationships (QSAR) with the six Merck-Serono inhibitors with a 2(Z)-2-(4-*tert*-butylthiazol-
214 2(3*H*)-ylidene)-2-(2-aminopyrimidin-4-yl) acetonitrile core structure. Creating the protein model
215 with the HOMOLOGY module of INSIGHTII (Accelrys Software, Inc., San Diego CA) was
216 straightforward since no insertions or deletions occur in the binding site. Molecular docking of
217 inhibitors was performed with the program FLO/QXP using Metropolis Monte Carlo procedures
218 (18). Inhibitors were treated as fully flexible as well as the side chains of amino acid residues in
219 the binding site.

220

221

222

Results

223 **Sequence analysis and RNA interference-** Two GSK-3 encoding genes were found in the *T. brucei*
224 genome by BLAST homology searches: a long version (Tb927.7.2420, encoding a predicted 501 amino
225 acid protein) and a short version (Tb10.61.3140 encoding a predicted 352 amino acid protein). Homology
226 comparisons do not reveal which homolog might be equivalent to GSK-3 α or GSK-3 β mammalian forms
227 (Table 1) and both the *Tbru*GSK-3 long and short versions are more homologous to human GSK-3 β than

228 to GSK-3 α . *Tbru*GSK-3 short or long mRNA knockdown was accomplished by over-expressing double
229 stranded RNA in mammalian blood stream form (BSF) of *T. brucei*. Two RNAi constructs were
230 separately tested to knock down the expression of the *Tbru*GSK-3 short gene. At 48 hrs, Northern
231 analysis demonstrated a 65% mRNA reduction for *Tbru*GSK-3 short construct 1 and a 76% mRNA
232 reduction for *Tbru*GSK-3 short construct 2 (Fig. 2). Along with the reduction of *Tbru*GSK-3 short
233 mRNA, induction of dsRNA led to striking inhibition of cell proliferation (Fig. 2). Induction of the
234 *Tbru*GSK-3 long RNAi construct yielded 82% mRNA knock-down of that gene (Fig. 2) but the inhibition
235 of growth was not as complete as that produced by the *Tbru*GSK short constructs (Fig. 2). Because of
236 the more pronounced growth inhibition by RNAi directed against *Tbru*GSK-3 short, we chose to focus
237 further work on the *Tbru*GSK-3 short enzyme.

238
239 **Southern blot analysis-** Hybridizing a Southern blot membrane with a radiolabeled GSK-3 short probe
240 (same sequence used for RNAi) revealed a single hybridizing band with four double restriction enzyme
241 digests to rule out a possible off target effect for the RNAi sequence. In each case, the MW of the
242 hybridizing band was predicted from the *Tbru*GSK-3 short genomic sequence (Fig. 3). The presence of a
243 single band for each digest at the predicted MW for *Tbru*GSK-3 short indicates that there is only one
244 complementary sequence to the RNAi segment used in the genome of *T. brucei*, and it is the *Tbru*GSK-3
245 short gene.

246
247 **Expression of highly-active recombinant *Tbru*GSK-3 short enzyme-** Recombinant *Tbru*GSK-3 short was
248 produced in *E. coli* as a C-terminal fusion with maltose binding protein (MBP) (Fig. 4), because non-
249 MBP-fused *Tbru*GSK-3 short was insoluble in *E. coli*. The enzyme substrate Km for ATP was
250 determined to be 4.5 μ M while the Km for the phosphorylated peptide (GSP-2) was 2.4 μ M (Table 2).
251 The specific activity of the purified *Tbru*GSK-3 short enzyme was found to be 1000U/mg (where 1 U was
252 defined as the incorporation of 1 nM phosphate into 1.2 μ M GSP-2 per minute at 30°C at a final ATP

253 concentration of 1.2 μM), comparable to 922U/mg cited for commercially-available human GSK-3 β (Lot
254 28407U, Upstate Cell Signaling Solutions, Temecula CA).

255
256 **Activity of kinase inhibitors against *Tbru*GSK-3 short and *T. brucei* BSF parasites-** Screening of 48
257 commercially-available protein kinase inhibitors has revealed GW8510 (Table 3) as a compound with 1
258 nM activity (IC_{50}) against the *Tbru*GSK-3 short enzyme and about 100 nM activity (EC_{50}) against
259 bloodstream form *T. brucei*. We have also identified other compounds as shown in Table 3 with activity
260 against the enzyme, but they may be inhibiting additional targets in the *T. brucei* cells as suggested by
261 comparatively low EC_{50} values in comparison to their IC_{50} values. In a screen against 255 compounds
262 with known activity against human GSK-3 β . (Merck-Serono, Geneva, Switzerland.), we observed a
263 correlation between enzyme and cellular activity which supports the chemical validation of *Tbru*GSK as a
264 drug target (examples shown in Table 4). Compounds of this series that inhibit *Tbru*GSK enzyme and
265 that inhibit *T. brucei* BSF growth demonstrate an excellent correlation between enzyme inhibition and
266 cell growth inhibition. Further research is required to establish if the identified “hit” compounds kill *T.*
267 *brucei* cells by specifically inhibiting GSK-3 short, but the data support chemical validation of GSK-3
268 short as a drug target for *T. brucei*.

269
270 **Model of *T. brucei* GSK-3 with Merck-Serono inhibitors-** A homology model of *Tbru*GSK-3 short was
271 constructed on the basis of a crystal structure of the human GSK-3 β enzyme in complex with an inhibitor.
272 Subsequently the six Merck-Serono inhibitors listed in Table 4 were docked to validate the model through
273 SAR. A linear regression between the predicted binding energies and experimental energies derived from
274 the IC_{50} 's shows an excellent correlation ($r^2 = 0.85$, $n=6$ and $F=23.3$ which indicates
275 a significance level of 99.0%) (Fig. 5). The predicted binding mode of the 30 nM Merck-Serono inhibitor
276 2 is shown in Figure 6. It features double hydrogen bond recognition pattern typical for many kinase
277 inhibitors involving the 2-amino-pyrimidinyl group of the inhibitor and a consecutive hydrogen bond
278 donor and acceptor from the protein backbone. Several hydrophobic contacts are present between the

279 thiazolyl and Cys 170 as well as Phe 31 originating from the glycine rich loop characteristic for kinases,
280 the nitrile and the “gatekeeper” residue Met 101, and the pyrimidinyl and Leu 159. The N-methyl-
281 piperidinyl makes a hydrogen bond to the carbonyl of Pro 105, and is further enveloped by Phe 103 and
282 Arg 110, which is in a salt bridge with Glu 106. Comparing the human structure and the model of the *T.*
283 *brucei* structure, it is predicted that specificity can be found with GSK-3 kinase inhibitors because of
284 differences in seven residues in the binding site (Table 6).

285

286

Discussion

287 In this paper, we report genetic and chemical validation data to support the hypothesis that
288 *Tbru*GSK-3 short is a drug target for *T. brucei*. First, RNAi experiments targeting the *Tbru*GSK-3 short
289 demonstrates dramatic growth inhibition of *T. brucei* bloodstream forms. It is likely that the RNAi
290 construct inhibits only the target *Tbru*GSK-3 short gene because Southern analysis probing with the same
291 DNA fragment used for the RNAi, showed only a single hybridizing band (in 4 separate digests) with
292 the molecular weight expected for the *Tbru*GSK-3 short gene. Thus, there was insufficient nucleotide
293 identity for cross hybridization by Southern analysis. Furthermore, the nucleotide sequence of *Tbru*GSK
294 short RNAi construct has only 47% identity to the corresponding region of *Tbru*GSK long with no
295 stretches of nucleotide identity longer than 11 bases, indicating that it is unlikely that the *Tbru*GSK-3
296 short RNAi would affect *Tbru*GSK-3 long expression. Therefore, it is very likely that the RNAi causes
297 only the specific effect on *Tbru*GSK-3 short gene expression. This also suggests that the growth
298 inhibitory effect of *Tbru*GSK-3 short RNAi occurs independently of *Tbru*GSK-3 long inhibition and that
299 *Tbru*GSK-3 short and long have non-overlapping functions that cannot be complemented by one another.
300 Second, a series of kinase inhibitors directed against GSK-3 correlated well in their anti-BSF cellular
301 activity and their activity against *Tbru*GSK-3 short enzyme. We cannot exclude the possibility that these
302 compounds inhibit targets in the cell other than GSK-3, and thus could exert their effects by the additive
303 actions. For instance, it is known that many GSK-3 inhibitors also inhibit cyclin-dependent kinases
304 (CDK) 1 and 2 (11, 31), which have a very similar active site to GSK-3 (27). Inhibition of CDKs has been

305 shown to arrest the growth of *T. brucei* (12, 13, 31). Recombinant CDK homologs enzymes are not
306 currently available from *T. brucei* due to difficulty with heterologous expression of these proteins, thus
307 we have been unable to test for cross-activity of the compounds to the CDKs. It is likely that many
308 kinase inhibitors act on targets other than *Tbru*GSK-3 short to inhibit BSF cell growth, as some protein
309 kinase inhibitors effectively impaired cells growth but had little activity against *Tbru*GSK-3 short.
310 However, there is a strong correlation between *Tbru*GSK-3 short enzyme activity and BSF cell
311 proliferation inhibition. Thus the chemical and genetic evidence favors that *Tbru*GSK-3 short is a good
312 target for drugs against *T. brucei*.

313 The ability to selectively target the *Tbru*GSK-3 enzymes over the mammalian GSK-3 orthologs
314 may be important to avoid toxicity caused by effects on cell signaling and cell cycle regulation. Human
315 GSK-3 β and *Tbru*GSK-3 short are only 41% identical and thus it seems possible that selective inhibitors
316 of *Tbru*GSK-3 short can be found. Indeed, the molecular modeling studies show active site differences
317 that should be possible to translate to selective inhibition. An example of potential selectivity from this
318 study is that one of the interactions of the Merck-Serono inhibitors is predicted to be with Met 101 of
319 *Tbru*GSK-3 short, which is a Leu in human GSK-3 β . We are pursuing crystallographic structure
320 determination of *Tbru*GSK-3 short complexed with inhibitors, but it has been difficult to cleave MBP
321 from the *Tbru*GSK-3 short, separate non-phosphorylated from phosphorylated protein, and have sufficient
322 protein for crystallization trials. Future studies will include continued attempts to solve the 3-D structure
323 as well as high-throughput screening against *Tbru*GSK-3 short and human GSK-3 β to find compounds
324 that show selectivity for *Tbru*GSK-3 short.

325

326 **Acknowledgements**

327 The authors would like to acknowledge the key collaborations were initiated by Dr Solomon Nwaka,
328 TDR, who continues to advise us in the project. The authors also wish to acknowledge the support of
329 Professor Wim Hol and the entire [Medical Structural Genomics of Pathogenic Protozoa](#) group who
330 initiated the cloning and characterization of *Tbru*GSK-3 short. Funding was from UNICEF/UNDP/World

331 Bank/WHO Special Programme for Research and Training in Tropical Diseases (TDR) and an
332 unrestricted grant from Merck-Serono.

ACCEPTED

333
334
335
336
337
338
339
340
341
342
343
344
345
346
347
348
349
350
351
352
353
354
355
356
357

References

1. **Alexandrov, A., M. Vignali, D. J. LaCount, E. Quartley, C. de Vries, D. De Rosa, J. Babulski, S. F. Mitchell, L. W. Schoenfeld, S. Fields, W. G. Hol, M. E. Dumont, E. M. Phizicky, and E. J. Grayhack.** 2004. A facile method for high-throughput co-expression of protein pairs. *Mol.Cell Proteomics*. **3**:934-938.
2. **Alibu, V. P., L. Storm, S. Haile, C. Clayton, and D. Horn.** 2005. A doubly inducible system for RNA interference and rapid RNAi plasmid construction in *Trypanosoma brucei*. *Mol.Biochem.Parasitol*. **139**:75-82.
3. **Allocco, J. J., R. Donald, T. Zhong, A. Lee, Y. S. Tang, R. C. Hendrickson, P. Liberator, and B. Nare.** 2006. Inhibitors of casein kinase 1 block the growth of *Leishmania major* promastigotes in vitro. *Int.J.Parasitol*. **36**:1249-1259.
4. **Barbu, V. and F. Dautry.** 1989. Northern blot normalization with a 28S rRNA oligonucleotide probe. *Nucleic Acids Res.* **17**:7115.
5. **Copeland, R. A., D. L. Pompliano, and T. D. Meek.** 2006. Drug-target residence time and its implications for lead optimization. *Nat.Rev.Drug Discov.* **5**:730-739.
6. **Dajani, R., E. Fraser, S. M. Roe, N. Young, V. Good, T. C. Dale, and L. H. Pearl.** 2001. Crystal structure of glycogen synthase kinase 3 beta: structural basis for phosphate-primed substrate specificity and autoinhibition. *Cell* **105**:721-732.
7. **Droucheau, E., A. Primot, V. Thomas, D. Mattei, M. Knockaert, C. Richardson, P. Sallicandro, P. Alano, A. Jafarshad, B. Baratte, C. Kunick, D. Parzy, L. Pearl, C. Doerig, and L. Meijer.** 2004. *Plasmodium falciparum* glycogen synthase kinase-3: molecular model, expression, intracellular localisation and selective inhibitors. *Biochim.Biophys.Acta* **1697**:181-196.
8. **Eswaran, J., Lee, W.H., Debreczeni, J.E., Filippakopoulos, P., Turnbull, A., Fedorov, O., Deacon, S.W., Peterson, J.R. and Knapp, S.** 2007. Crystal Structures of the p21-activated

- 358 kinases PAK4, PAK5, and PAK6 reveal catalytic domain plasticity of active group II PAKs.
359 Structure. **15**: 201-213.
- 360 9. **Fairlamb, A. H.** 2003. Chemotherapy of human African trypanosomiasis: current and future
361 prospects. Trends Parasitol. **19**:488-494.
- 362 10. **Frame, S. and P. Cohen.** 2001. GSK3 takes centre stage more than 20 years after its discovery.
363 Biochem.J. **359**:1-16.
- 364 11. **Grant, K.M., Dunion, M.H., Yardley, V., Skaltsounis, A.L., Marko, D., Eisenbrand, G.,**
365 **Croft, S.L., Meijer, L. and Mottram, J.C.** 2004. Inhibitors of *Leishmania mexicana* CRK3
366 cyclin-dependent kinase: chemical library screen and antileishmanial activity. Antimicrob.
367 Agents Chem. **48**:3033-3042.
- 368 12. **Hammarton, T.C., Clark, J., Douglas, F., Boshart, M., and Mottram, J.C.** 2003. Stage-
369 specific differences in cell cycle control in *Trypanosoma brucei* revealed by RNA interference of
370 a mitotic cyclin, J Biol Chem. **278**: 22877-22886.
- 371 13. **Hammarton, T.C, Engstler, M., and Mottram, J.C.** 2004. The *Trypanosoma brucei* cyclin,
372 CYC2, is required for cell cycle progression through G1 phase and for maintenance of procyclic
373 form cell morphology. J Biol Chem; **279**:24757-24764.
- 374 14. **Hammarton, T. C., Mottram J. C., and Doerig C.** 2003. The cell cycle of parasitic protozoa:
375 potential for chemotherapeutic exploitation. Prog.Cell Cycle Res. **5**:91-101.
- 376 15. **Hirumi, H. and K. Hirumi.** 1989. Continuous cultivation of *Trypanosoma brucei* blood stream
377 forms in a medium containing a low concentration of serum protein without feeder cell layers.
378 J.Parasitol. **75**:985-989.
- 379 16. **Johnson, K., Liu, L., Majdzadeh, N., Chavez, C., Chin, P.C., Morrison, B., Wang, L., Park,**
380 **J., Chugh, P., Chen, H.M. and D'Mello, S.R.** 2005. Inhibition of neuronal apoptosis by the
381 cyclin-dependent kinase inhibitor GW8510: identification of 3' substituted indolones as a
382 scaffold for the development of neuroprotective drugs. J Neurochem. **93**:538-548.

- 383 17. **Kunick, C., Zeng, Z., Gussio, R., Zaharevitz, D., Leost, M., Totzke, F., Schächtele, C.,**
384 **Kubbutat, M.H.G., Meijer, L. and Lemcke, T.** 2005. Structure-Aided Optimization of Kinase
385 Inhibitors Derived from Alsterpaullone. **ChemBioChem**. **6: 541-549.**
- 386 18. **Liao, J. J.** 2007. Molecular recognition of protein kinase binding pockets for design of potent and
387 selective kinase inhibitors. *J.Med.Chem.* **50:409-424.**
- 388 19. **McMartin, C. and R. S. Bohacek.** 1997. QXP: powerful, rapid computer algorithms for
389 structure-based drug design. *J.Comput.Aided Mol.Des* **11:333-344.**
- 390 20. **Medina-Acosta, E. and G. A. Cross.** 1993. Rapid isolation of DNA from trypanosomatid
391 protozoa using a simple 'mini-prep' procedure. *Mol.Biochem.Parasitol.* **59:327-329.**
- 392 21. **Mehlin, C., E. Boni, F. S. Buckner, L. Engel, T. Feist, M. H. Gelb, L. Haji, D. Kim, C. Liu,**
393 **N. Mueller, P. J. Myler, J. T. Reddy, J. N. Sampson, E. Subramanian, W. C. Van Voorhis,**
394 **E. Worthey, F. Zucker, and W. G. Hol.** 2006. Heterologous expression of proteins from
395 *Plasmodium falciparum*: results from 1000 genes. *Mol.Biochem.Parasitol.* **148:144-160.**
- 396 22. **Meijer, L., M. Flajolet, and P. Greengard.** 2004. Pharmacological inhibitors of glycogen
397 synthase kinase 3. *Trends Pharmacol.Sci.* **25:471-480.**
- 398 23. **Naula, C., M. Parsons, and J. C. Mottram.** 2005. Protein kinases as drug targets in
399 trypanosomes and *Leishmania*. *Biochim.Biophys.Acta* **1754:151-159.**
- 400 24. **Pearson, W. R. and D. J. Lipman.** 1988. Improved tools for biological sequence comparison.
401 *Proc.Natl.Acad.Sci.U.S.A* **85:2444-2448.**
- 402 25. **Pink, R., A. Hudson, M. A. Mouries, and M. Bendig.** 2005. Opportunities and challenges in
403 antiparasitic drug discovery. *Nat.Rev.Drug Discov.* **4:727-740.**
- 404 26. **Plyte, S. E., K. Hughes, E. Nikolakaki, B. J. Pulverer, and J. R. Woodgett.** 1992. Glycogen
405 synthase kinase-3: functions in oncogenesis and development. *Biochim.Biophys.Acta* **1114:147-**
406 **162.**
- 407 27. **Polychronopoulos, P., Magiatis, P., Skaltsounis, A.L., Myrianthopoulos, V., Mikros, E.,**
408 **Tarricone, A., Musacchio, A., Roe, S.M., Pearl, L., Leost, M., Greengard, P. and Meijer, L.**

- 409 2004. Structural basis for the synthesis of indirubins as potent and selective inhibitors of
410 glycogen synthase kinase-3 and cyclin-dependent kinases. *J Med Chem.* **47**:935-946.
- 411 28. **Raz, B., M. Iten, Y. Grether-Buhler, R. Kaminsky, and R. Brun.** 1997. The Alamar Blue
412 assay to determine drug sensitivity of African trypanosomes (*T.b. rhodesiense* and *T.b.*
413 *gambiense*) in vitro. *Acta Trop.* **68**:139-147.
- 414 29. **Redmond, S., J. Vadivelu, and M. C. Field.** 2003. RNAit: an automated web-based tool for the
415 selection of RNAi targets in *Trypanosoma brucei*. *Mol.Biochem.Parasitol.* **128**:115-118.
- 416 30. **Stambolic, V. and J. R. Woodgett.** 1994. Mitogen inactivation of glycogen synthase kinase-3
417 beta in intact cells via serine 9 phosphorylation. *Biochem.J.* **303**:701-704.
- 418 31. **Tu, X. and Wang, C.C.** 2005. Pairwise Knockdowns of cdc2-Related Kinases (CRKs) in
419 *Trypanosoma brucei* Identified the CRKs for G1/S and G2/M Transitions and Demonstrated
420 Distinctive Cytokinetic Regulations between Two Developmental Stages of the Organism.
421 *Eukaryot Cell.* **4**:755-764.
- 422 .
- 423 32. **Wang, Q. M., C. J. Fiol, A. A. DePaoli-Roach, and P. J. Roach.** 1994. Glycogen synthase
424 kinase-3 beta is a dual specificity kinase differentially regulated by tyrosine and serine/threonine
425 phosphorylation. *J.Biol.Chem.* **269**:14566-14574.
- 426 33. **Wirtz, E., S. Leal, C. Ochatt, and G. A. Cross.** 1999. A tightly regulated inducible expression
427 system for conditional gene knock-outs and dominant-negative genetics in *Trypanosoma brucei*.
428 *Mol.Biochem.Parasitol.* **99**:89-101.

429

Figure Legends

430 **Figure 1: Enzymatic action of GSK-3.** With most GSK-3 substrates, another (priming) kinase
431 first places a phosphate (PO₃) on a serine or threonine (S/T) residue separated by three amino
432 acids (X) in the carboxy direction to target S/T residues. Then GSK-3 phosphorylates target S/T
433 groups. Occasionally GSK-3 has been shown to phosphorylate non-primed peptide substrates
434 and has been shown to autophosphorylate GSK-3 on S/T or tyrosine (10,32).

435 **Figure 2: RNAi of *Tbru*GSK-3 homologs. top:** The graph shows the growth of *T. brucei* BSF
436 as days after tetracycline addition (day 0). *T. brucei* strain 427 “single marker” (SM) cells were
437 transfected with plasmids that with tetracycline administration, lead to the induction of dsRNA
438 resulting in RNAi inhibition of target gene expression. Both homologs of GSK-3 were
439 separately targeted, *Tbru*GSK-3 long and *Tbru*GSK-3 short (2 different constructs of *Tbru*GSK-3
440 short). SM cells served as a no-plasmid control. With the addition of tetracycline (+) dramatic
441 growth inhibition occurs compared with no-tetracycline control (-) when either the Long or Short
442 *Tbru*GSK-3 homologs are targeted. **Bottom:** The Northern blots shows reduction of mRNA
443 levels (Gene) for the *Tbru*GSK-3 short (S1 & S2) and *Tbru*GSK-3 long (L) transcripts with
444 tetracycline induction (+) vs. no tet (-). A tubulin mRNA control (Tub) differs little after RNAi
445 induction with tetracycline.

446 **Figure 3: Southern blot of *T. brucei* gDNA with *Tbru*GSK-3 short probe.** Genomic *T.*
447 *brucei* 427 SM DNA was digested, blotted, and probed with the RNAi region for the GSK1Short
448 (S1) to verify only a single band, corresponding to the *Tbru*GSK-3 short gene, hybridizes in the
449 *T. brucei* genome. Restriction digest predicted sizes are BamHI/PstI: 1702 bp; BamHI/AvaI:
450 2214 bp; NcoI/PstI: 2655 bp; NcoI/AvaI: 3167 bp.

451 **Figure 4:** Purity of recombinant *Tbru*GSK-3 short produced in *E. coli*. The enzyme was purified
452 by metal affinity chromatography followed by size exclusion chromatography. Shown are 3
453 lanes representing 25 μ g of protein from fractions (1-3) from size exclusion chromatography that
454 were pooled to make the working batch of enzyme for further study. Purity was judged greater
455 than 98%.

456 **Figure 5:** Correlation between experimental and predicted binding energies using the *Tbru*GSK-
457 3 short homology model. The R-square=0.85 and F=23.3, which indicates the linear relationship
458 is highly significant at the 99.0% level.

459 **Figure 6:** Model of the binding mode of Merck-Serono 2 (yellow) to *Tbru*GSK-3 short (made
460 with Pymol, DeLano Scientific LLC, San Carlos, CA, USA. <http://www.pymol.org>)
461

Table 1: Comparison of amino acid identities (%) of the two human orthologues of GSK-3 vs. *T. brucei* GSK-3 long and GSK-3 short. The smallest sum probability by BLASTP search is shown in parenthesis.

	huGSK-3 β	<i>Tbru</i> GSK-3 long	<i>Tbru</i> GSK-3 short
huGSK-3 α	67.4 (1 ^{e-177})	29.7 (2.2 ^{e-66})	35.6 (2.7 ^{e-82})
huGSK-3 β		33.1 (1.0 ^{e-71})	40.9 (9.1 ^{e-89})
<i>Tbru</i> GSK-3 long			30.6 (4.6 ^{e-66})

ACCEPTED

Table 2: Recombinant *T. brucei* Glycogen Synthase Kinase-3 short characteristics

Km		Specific activity*
ATP	Peptide (GSP-2)	
4.5 μ M	2.4 μ M	1000 U/mg

*1 U = incorporation of 1 nM phosphate into 1.2 μ M GSP-2 per minute at 30°C at an ATP concentration of 1.2 μ M.

ACCEPTED

Table 3: Commercial Kinase Inhibitors With Activity Against GSK Enzyme and *T. brucei* Bloodstream Forms (BSF) (selected from a panel of 48 kinase inhibitors)

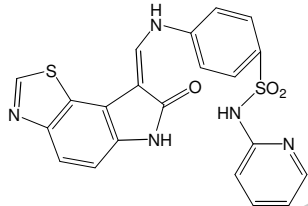
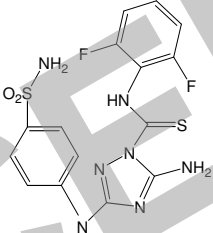
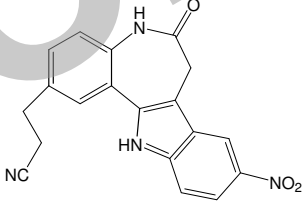
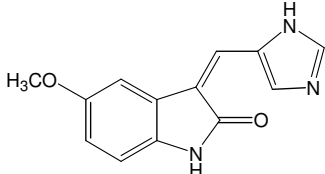
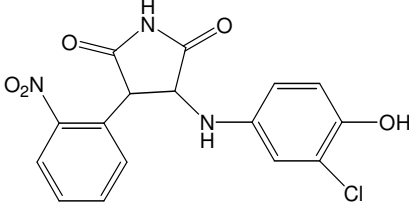
Compound	Structure	IC ₅₀ nM (<i>T. brucei</i> GSK Enzyme)	EC ₅₀ nM (<i>T. brucei</i> BSF growth assay)
GW8510		1	119
Cdk1/2 Inhibitor III		13	20
2-Cyanoethyl Alsterpaullone		336	150
SU9516		352	180
SB-415286		1000	740

Table 4: GSK-3 focused Inhibitors from Merck-Serono with Activity Against GSK Enzyme and *T. brucei* Bloodstream Forms (selected from a panel of 255 GSK-3 β inhibitors).

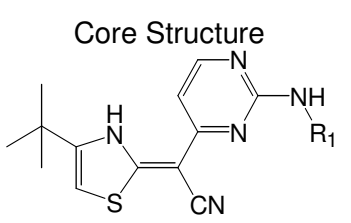
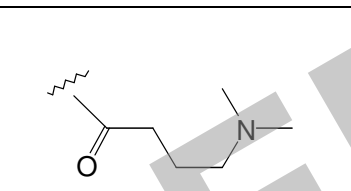
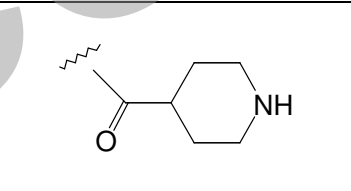
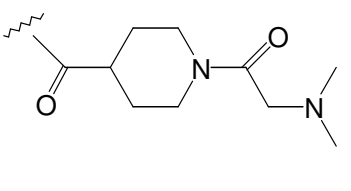

Core Structure			
Compound	R ₁	IC ₅₀ nM (<i>T. brucei</i> GSK Enzyme)	ED ₅₀ nM (<i>T. brucei</i> BSF growth assay)
1		4	50
2		30	65
3		46	200
4		22	410
5		30	458
6		168	705

Table 5. Oligonucleotide primers

No	ORF Position	Primer Description	Sequence 5'-3'
RNAi			
1	176-578	GSKshort1Fwd	CTGGATCCACCGAGAGTTGCAAATTATG
2		GSKshort1Rev	AAGGATCCTAGTAACGCGAGCAAATGTA
3	665-1056	GSKshort2Fwd	GTGGATCCTTCTTGGTGAACCGATATTC
4		GSKshort2Rev	TTGGATCCCTTCTTCAGCAGATACTCCC
5	159-531	GSKLongFwd	CCATGCGAGCAAGTGAGGTATG
6		GSKLongRev	GGCACTGGGATCAGAAGCGAAG
7	1013-1422	GSKLongprobe1*	CATCTGAGCGGGA ACTCTTCG
8		GSKLongprobe2*	CAGCCACGGTGGTAAAATCTC
GSK-3 protein Expression			
9	1-1059	<i>Tbru</i> GSKLICFwd	CTCACCACCACCACCACCATATGTCGCTCAACCTACCGATGC
10		<i>Tbru</i> GSKLICRev	ATCCTATCTTACTCACTTACTTCTTCAGCAGATACTCCCGC

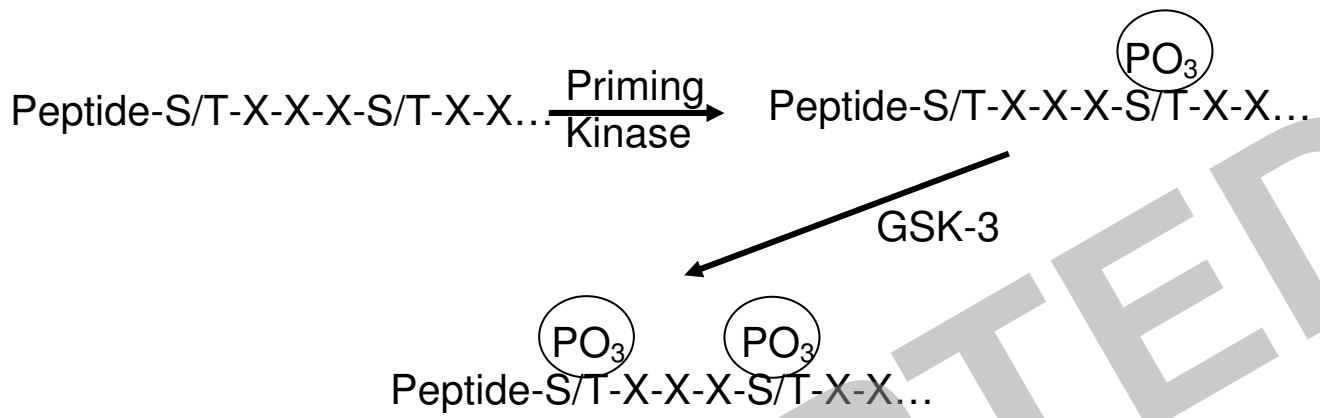
* Used as probes for Northern blot analysis of *Tbru*GSK-3 long

Table 6: Comparison of GSK-3 binding site residues ^a

T. brucei	Human		T. brucei	Human
V 25	V 61		M 101	L 132
A 26	I 62		E 102 *	* D 133
G 27	G 63		F 103	Y 134
Q 28 *	* N 64		V 104 *	* V 135
G 29	G 65		P 105	P 136
T 30	S 66		E 106	E 137
F 31	F 67		T 107	T 138
V 34	V 70		H 109	Y 140
L 36	Q 72		R 110	R 141
A 47	A 83		K 154	K 183
K 49	K 85		H 156	Q 185
E 61	E 97		N 157	N 186
M 65	M101		L 159	L 188
V 77	V110		C 170	C 199
			D 171	D 200

(^a) differing pairs in bold; (*) only backbone in binding site

Figure 1: Enzymatic action of GSK-3



ACCEPTED

Figure 2

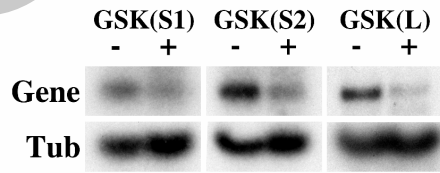
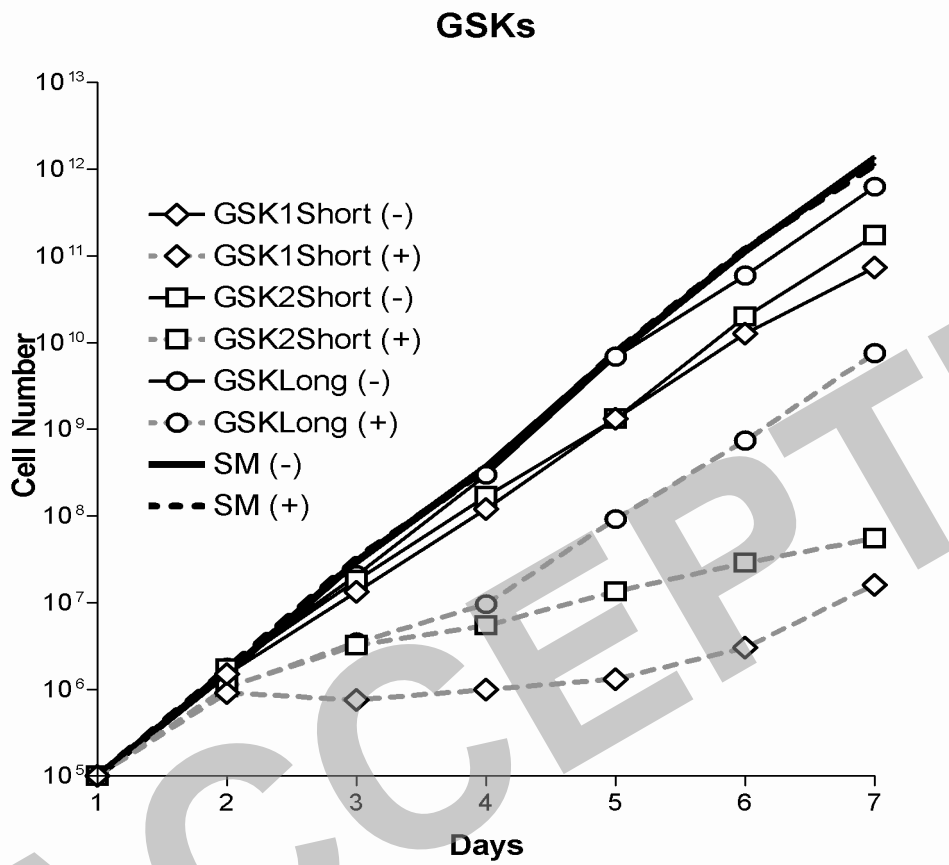


Figure 3
Southern blot probing with *Tbru*GSK-3 short demonstrates only one band per digest.

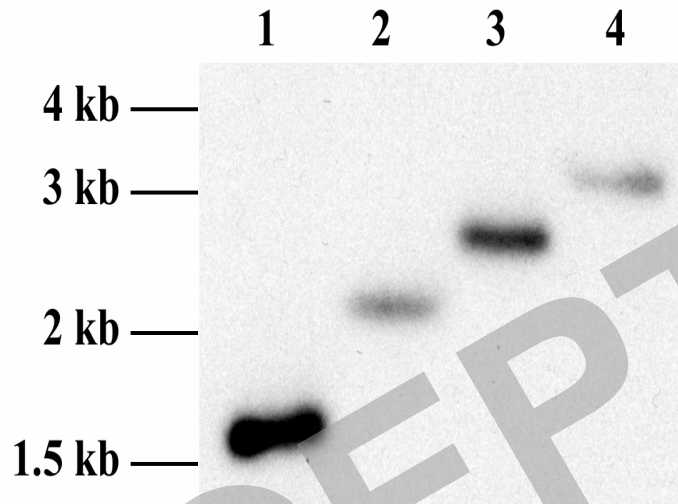
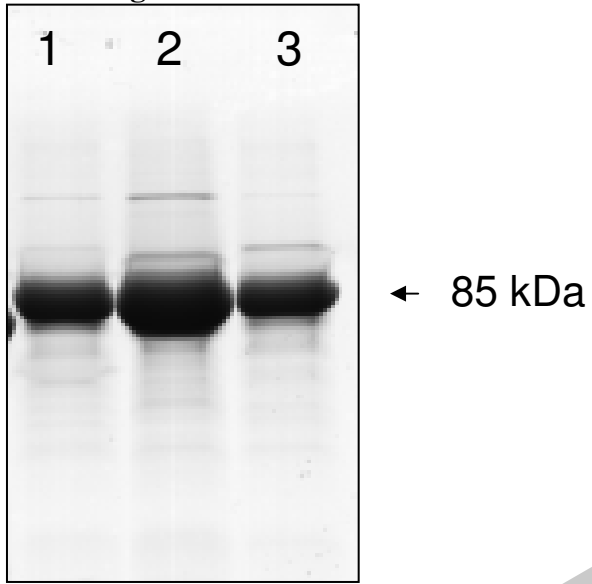


Figure 4



ACCEPTED

Figure 5

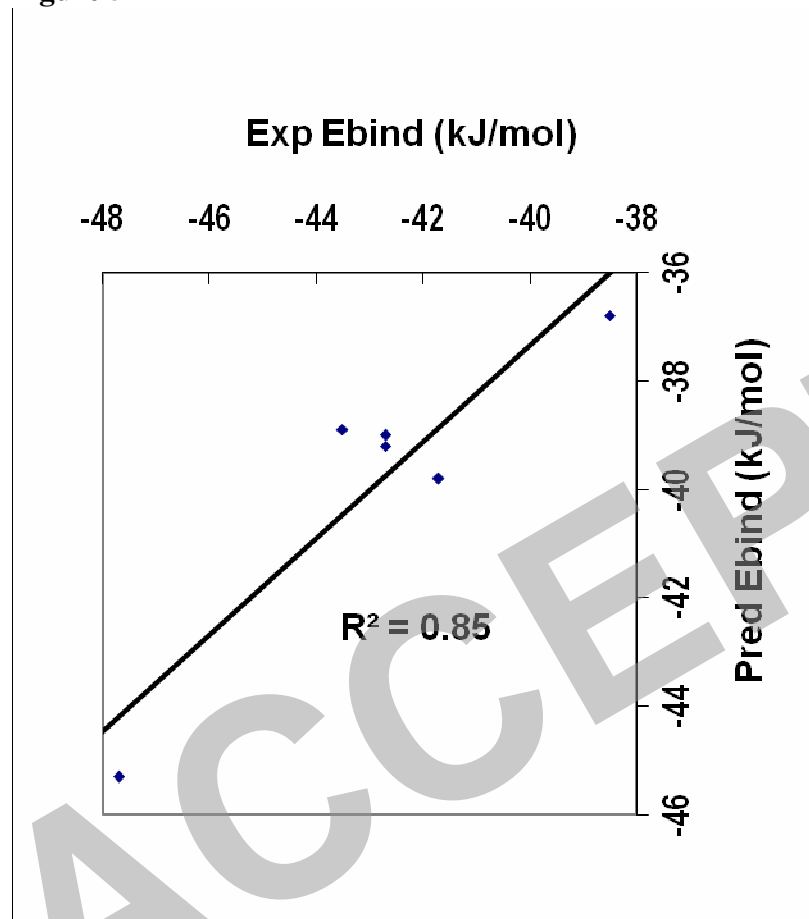


Figure 5: Correlation between experimental and predicted binding energies using the *T.brucei* homology model. The R-square=0.85 and F=23.3, which indicates the linear relationship is highly significant at the 99.0% level.

Figure 6

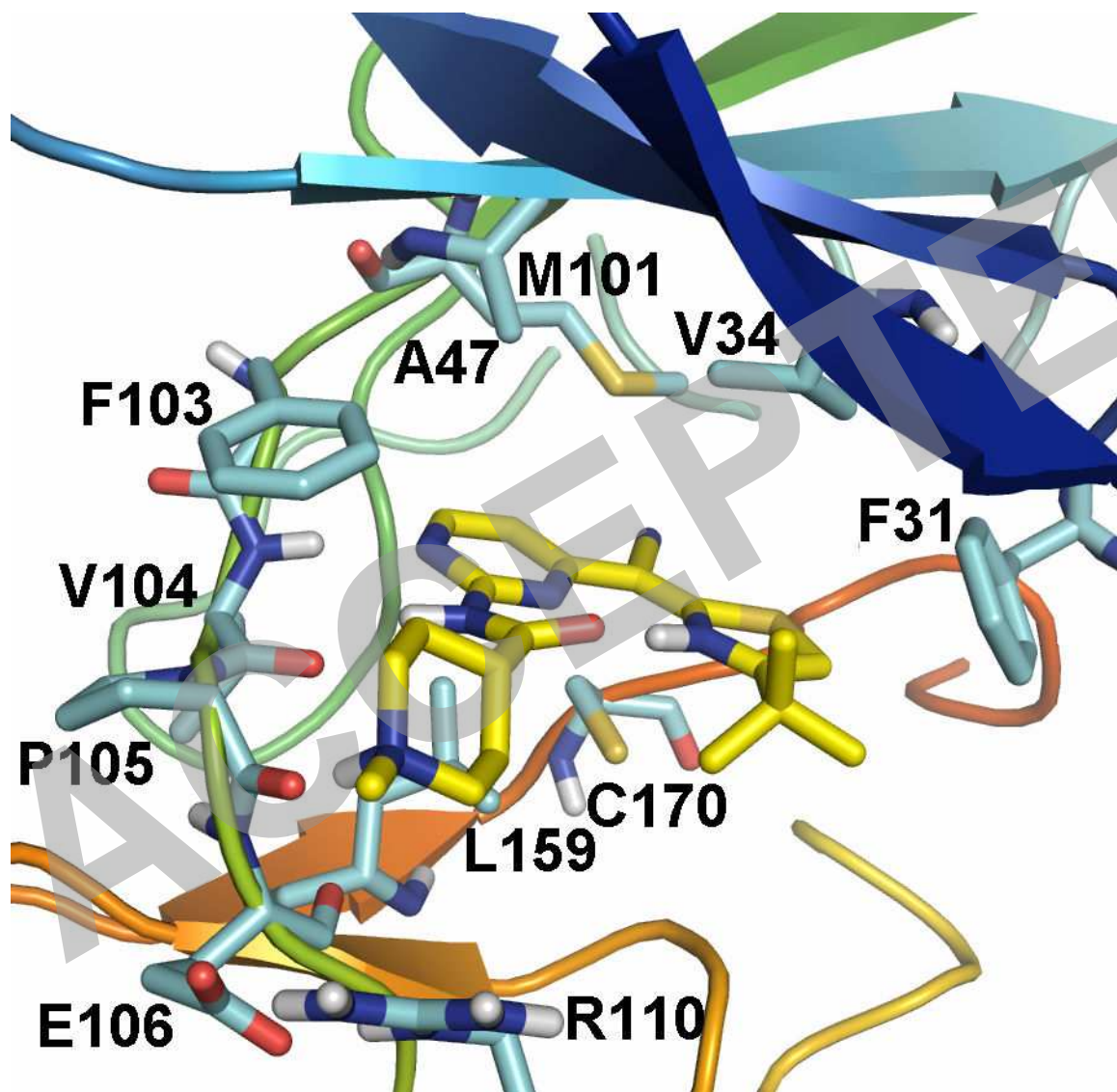


Figure 6: Model of the binding mode of Merck-Serono 2 (yellow) to *T. brucei* GSK-3 (made with Pymol, DeLano Scientific LLC, San Carlos, CA, USA. <http://www.pymol.org>)

